Received: 24 January 2021 | Revised: 1 June 2021 | Accepted: 3 June 2021

DOI: 10.1002/biot.202100043

Biotechnology Journal

RESEARCH ARTICLE

Microaerobic growth-decoupled production of α-ketoglutarate and succinate from xylose in a one-pot process using *Corynebacterium glutamicum*

Niklas Tenhaef[1,2] | **Jannick Kappelmann**[1,3] | **Arabel Eich**[1] | **Marc Weiske**[1] | **Lisette Brieß**[1] | **Christian Brüsseler**[1,2] | **Jan Marienhagen**[1,2,4] | **Wolfgang Wiechert**[1,2,5] | **Stephan Noack**[1,2]

[1] Institute of Bio- and Geosciences, IBG-1: Biotechnology, Forschungszentrum Jülich GmbH, Jülich, Germany

[2] Bioeconomy Science Center (BioSC), Forschungszentrum Jülich GmbH, Jülich, Germany

[3] Currenta GmbH & Co. OHG, Leverkusen, Germany

[4] Institute of Biotechnology, RWTH Aachen University, Aachen, Germany

[5] Computational Systems Biotechnology (AVT.CSB), RWTH Aachen University, Aachen, Germany

Correspondence
Stephan Noack, Institute of Bio- and Geosciences, IBG-1: Biotechnology, Forschungszentrum Jülich GmbH, Jülich D-52425, Germany.
Email: s.noack@fz-juelich.de

Abstract

Background: Lignocellulosic biomass is the most abundant raw material on earth. Its efficient use for novel bio-based materials is essential for an emerging bioeconomy. Possible building blocks for such materials are the key TCA-cycle intermediates α-ketoglutarate and succinate. These organic acids have a wide range of potential applications, particularly in use as monomers for established or novel biopolymers. Recently, *Corynebacterium glutamicum* was successfully engineered and evolved towards an improved utilization of D-xylose via the Weimberg pathway, yielding the strain WMB2$_{evo}$. The Weimberg pathway enables a carbon-efficient C5-to-C5 conversion of D-xylose to α-ketoglutarate and a shortcut route to succinate as co-product in a one-pot process.

Methods and Results: *C. glutamicum* WMB2$_{evo}$ was grown under dynamic microaerobic conditions on D-xylose, leading to the formation of comparably high amounts of succinate and only small amounts of α-ketoglutarate. Subsequent carbon isotope labeling experiments verified the targeted production route for both products in *C. glutamicum* WMB2$_{evo}$. Fed-batch process development was initiated and the effect of oxygen supply and feeding strategy for a growth-decoupled co-production of α-ketoglutarate and succinate were studied in detail. The finally established fed-batch production process resulted in the formation of 78.4 mmol L^{-1} (11.45 g L^{-1}) α-ketoglutarate and 96.2 mmol L^{-1} (11.36 g L^{-1}) succinate.

Conclusion: The developed one-pot process represents a promising approach for the combined supply of bio-based α-ketoglutarate and succinate. Future work will focus on tailor-made down-stream processing of both organic acids from the fermentation broth to enable their application as building blocks in chemical syntheses. Alternatively, direct conversion of one or both acids via whole-cell or cell-free enzymatic approaches

can be envisioned; thus, extending the network of value chains starting from cheap and renewable D-xylose.

KEYWORDS
α-ketoglutarate, *Corynebacterium glutamicum*, succinate, Weimberg pathway, xylose

1 | INTRODUCTION

Lignocellulosic biomass is the most abundant raw material and potential waste stream on earth.[1,2] To be integrated into existing value chains, it needs to be converted into chemical building blocks, versatile molecules that can be combined into more complex products. Sustainable production of such chemical building blocks increases the sustainability of the entire production chain. Organic acids are promising candidates for this concept, as they can be produced by microbial processes and have versatile functional groups.[3]

The oxocarboxylic acid α-ketoglutarate can be used as a dietary supplement,[4] in the synthesis of active pharmaceutical ingredients,[5,6] and to form biodegradable elastomers.[7] Currently, it is mainly produced by chemical synthesis from succinic acid and oxalic acid diethyl esters with a yield of 75%.[6] These processes use hazardous chemicals such as cyanohydrines or acyl cyanides and produce toxic waste. Bioprocesses using bacterial and yeast strains have been developed to provide more sustainable alternatives.[5] In terms of titer and yield, processes using the yeast *Yarrowia lipolytica* as production host and rapeseed oil as substrate show the best performance. Here, titers of up to 134 g L^{-1} and yields of up to 1.3 g g^{-1} were achieved.[5,8] Using *Corynebacterium glutamicum* as production host, titers of up to 5 g L^{-1} were achieved in a patent by inactivating the enzyme glutamate dehydrogenase and using a production medium with excess ammonium.[9]

The dicarboxylic acid succinate is currently used as chelator, surfactant, additive in the agricultural and food industries, in the pharmaceutical industry, and as a precursor molecule for numerous applications in the chemical industry.[10,11] Prominent examples of the latter application are the synthesis of tetrahydrofuran[12] and the esterification with 1,4-butanediol to provide the thermoplastic polymer polybutylene succinate.[13] A variety of bioprocesses for the production of succinate have been described.[14–19] Most of them use refined D-glucose or glycerol as feedstocks. Titers as high as 134 g L^{-1} have been achieved using *C. glutamicum* as the production host.[14] Recent studies also focused on the use of lignocellulosic biomass.[20] Here, specialized production hosts such as *Actinobacillus succinogenes* were used to utilize corn fiber hydrolysate and titers of 35.4 g L^{-1} were reached.[21]

Most processes for organic acid production rely on D-glucose or glycerol as substrate. The substrate is utilized via glycolysis and passed through the tricarboxylic acid (TCA) cycle, for example, to form α-ketoglutarate. This mode inevitably results in carbon losses during the conversion of D-isocitrate to α-ketoglutarate. The Weimberg pathway represents a promising, carbon-efficient alternative: First discovered in the bacterium *Pseudomonas fragi*,[22] this pathway theoretically allows C5-to-C5 conversion of D-xylose to α-ketoglutarate without carbon loss. D-xylose is an abundant carbohydrate in lignocellulosic biomass and one of the most abundant raw materials on earth.[23] Utilizing this carbohydrate instead of D-glucose, issues such as competition over arable land can be avoided.[24,25]

The gram-positive bacterium *C. glutamicum* is an established host for the production of organic acids. High titers have been achieved, for example, for succinate (1.1 mol L^{-1},[14]) and lactate (1.3 mol L^{-1},[26]). These processes are usually performed under microaerobic or anaerobic conditions to foster carbon flux into such products, those formation is coupled to the recycling of reduced cofactors (e.g., NADH and MQH_2 in *C. glutamicum*) when oxidative phosphorylation becomes limiting.

Recently, the Weimberg pathway was introduced into *C. glutamicum*. A codon-optimized version of the *xylXABCD* genes encoding the relevant enzymes of the Weimberg pathway from *Caulobacter crescentus* were cloned into an appropriate vector system and transformed into *C. glutamicum* to allow growth on D-xylose as sole carbon and energy source.[27] Adaptive Laboratory Evolution (ALE) was used to increase substrate uptake and growth rates, yielding strain $WMB2_{evo}$.[28] Using the findings from the ALE study, several rational engineered strains were constructed. The strain *C. glutamicum* P_{O6} *iolT1* Δ*odhA* pEKEx3-*xylXD*$_{Cc}$-opt was able to accumulate 7.92 ± 0.13 g L^{-1} α-ketoglutarate.[29]

In this study, the ability of strain $WMB2_{evo}$ for combined production of α-ketoglutarate and succinate from D-xylose under microaerobic conditions is demonstrated. To verify the direct conversion of D-xylose to α-ketoglutarate and succinate via the Weimberg pathway in this strain, a comparative ^{13}C-labeling experiment was employed. Specifically, 1-^{13}C-D-xylose was applied as isotopic tracer and the enrichment patterns in metabolites of central carbon metabolism of strain $WMB2_{evo}$ were compared to a *C. glutamicum* strain harboring the well-known isomerase pathway for D-xylose utilization. The effect of oxygen limitation on co-production was investigated in fed-batch bioreactor cultures. Finally, by choosing a robust microaerobic condition, the established one-pot process was further intensified by applying higher substrate concentrations in an optimal feeding scheme.

2 | MATERIAL AND METHODS

2.1 | Bacterial strains, growth media, and cryo-conservation

The strain *C. glutamicum* pEKEx3-*xylXABCD*$_{Cc}$-opt ($WMB2_{evo}$) underwent adaptive laboratory evolution as described recently [28] and the strain *C. glutamicum* pEKEx3-*xylA*$_{Xc}$ -*xylB*$_{Cg}$ (ISO) [30] were used in this study.

If not stated otherwise, all chemicals were of analytical grade and purchased from Sigma (Steinheim, Germany), Merck (Darmstadt, Germany) or Roth (Karlsruhe, Germany).

Complex BHI medium was prepared by dissolving 37 g L^{-1} brain-heart infusion (BHI) in deionized water, followed by autoclaving at 121°C for 20 min.

Defined CGXII medium [31] containing per liter of deionized water 20 g $(NH_4)_2SO_4$, 1 g K_2HPO_4, 1 g KH_2PO_4, 13.25 mg $CaCl_2{\cdot}2H_2O$, 0.25 g $MgSO_4{\cdot}7H_2O$, 10 mg $FeSO_4{\cdot}7H_2O$, 10 mg $MnSO_4{\cdot}H_2O$, 0.02 mg $NiCl_2{\cdot}6H_2O$, 0.313 mg $CuSO_4{\cdot}5H_2O$, 1 mg $ZnSO_4{\cdot}7H_2O$, 0.2 mg biotin, 30 mg 3,4-dihydroxybenzoate (PCA) and 100 mg isopropyl β-D-thiogalactoside (IPTG). When shake flasks were used for cultivation, 5 g urea and 42 g 3-(*N*-morpholino)propanesulfonic acid (MOPS) were added. D-glucose or D-xylose was added in varying amounts dependent on the respective experiment.

All strains were kept as cryo-stocks at -80°C. For generation of new cryo-stocks, a shake flask cultivation in defined CGXII was done overnight. Cells were centrifuged at 4000 g for 10 min, resuspended in 0.9% (w v^{-1}) sodium chloride + 20% (v v^{-1}) glycerol and subsequently stored at -80°C.

2.2 | Shake flask and bioreactor cultivations

For shake flask cultivations, flasks with three baffles and a volume of 1 L, filled with 100 mL medium, were used. Flasks were shaken in an incubator at 250 rpm and 30°C. Inoculation was done from cryo-cultures to a starting OD_{600} of 0.1. Samples for cold methanol quenching (see below) were taken from the mid-exponential phase, determined by OD measurement.

Bioreactor cultivations were done in a parallel cultivation platform (Eppendorf/DASGIP, Jülich, Germany) using 3.8 L glass vessels. If not stated otherwise, the vessels were inoculated from an exponential growing shake flask culture to a final OD_{600} of 1. A pH of 7 was maintained during the cultivation by feeding 5 M H_3PO_4 and 5 M NH_4OH on demand. If not stated otherwise, temperature and air flow were set to 30°C and 0.5 vvm, respectively. Online measurements were taken for pH (405-DPAS-SC-K80/225, Mettler Toledo), DO (Visiferm DO 225, Hamilton) and exhaust gas composition (GA4, DASGIP AG). Aerobic process conditions were maintained by controlling the stirrer speed (400 — 1200 rpm) to achieve a dissolved oxygen concentration (DO) of at least 30%. Microaerobic process conditions were achieved by setting a constant stirrer speed and varying the oxygen content in the inlet gas by adding nitrogen (exact values given for each experiment).

2.3 | Biomass quantification methods

Depending on the experiment, one or more of the following biomass quantification methods were used:

Optical density at a wavelength of 600 nm was measured using a UV-spectrophotometer (UV-1800, Shimadzu) and 1 mL cuvettes. 0.9% (w v^{-1}) NaCl solution was used as a reference. Absorption of samples was ensured to be between 0.05 and 0.3 a. u. by dilution. If not stated otherwise, measurements were done in analytical triplicates.

Cell dry weight was determined by transfer of a 2 mL cultivation sample in a pre-dried and pre-weight tube. The sample was centrifuged for 10 min at 13,000 × *g* in a tabletop centrifuge. Subsequently, the supernatant was removed, and the pellet was washed using 1 mL 0.9% (w v^{-1}) NaCl solution. The sample was centrifuged again for 10 min at 13,000 × *g* in a tabletop centrifuge and the supernatant discarded. The sample was dried in a dry oven at 80°C for 12 to 24 h and subsequently weight.

2.4 | Quantification of D-xylose in culture supernatant

D-Xylose concentration was quantified by an enzymatic assay (D-Xylose Assay Kit, Megazyme, Wicklow, Ireland). The protocol used was modified: One well of a 96-well plate contained 290 μL master mix and 10 μL sample or standard. Seven standard concentrations were measured to cover the linear range of 0.1 to 1 g L^{-1}. Master mix for one MTP consisted of 32 mL TRIS-maleate buffer (pH 6.8), 1 mL 100 mM $MgCl_2$ solution, 0.5 mL 50 g L^{-1} NAD solution and 0.1 mL XDH/XMR solution (from kit). After incubation for 30 min, absorption at 340 nm was measured using an Infinite 200 microplate reader (Tecan, Switzerland). External standards were used for linear regression within the linear dynamic range. Estimation of measurement errors was done by parametric bootstrapping as previously described.[32]

2.5 | Quantification of organic acids in culture supernatant

Samples were prepared by passing the supernatants through a cellulose acetate syringe filter (0.2 μm, DIA-Nielsen, Düren, Germany).

Concentrations of carbohydrates were measured by high performance liquid chromatography (Agilent 1100 Infinity, Agilent Technologies, Santa Clara, CA) using isocratic ion exchange on an Organic Acid Resin HPLC Column 300 × 8 mm (CS Chromatography, Düren, Germany) as stationary phase and 0.1 M H_2SO_4 as mobile phase with a flow rate of 0.6 mL min^{-1}. The column temperature was 80°C and the injection volume 10 μL. Carbohydrates were detected using a refractive index detector.

Concentrations of succinate and α-ketoglutarate were measured by high performance liquid chromatography (Agilent 1100 Infinity, Agilent Technologies, Santa Clara, CA) using isocratic ion exchange on an Organic Acid Resin HPLC Column 300 × 8 mm (CS Chromatography, Düren, Germany) as stationary phase and 0.1 M H_2SO_4 as mobile phase with a flow rate of 0.6 mL min^{-1}. The column temperature was 45°C and the injection volume 100 μL. Components were detected using UV light absorption at 215 nm with a diode array detector.

For external calibration, standards of organic acids or carbohydrates (supplied by Sigma-Aldrich, Steinheim, Germany) were applied in the

linear dynamic range. Estimation of measurement errors was done by parametric bootstrapping as previously described.[32]

2.6 | Analysis of ^{13}C-labeled intermediates

Each sampled biomass pellet was processed and extracted following the procedure described previously.[33] Cell extracts were separated on an Agilent 1260 Infinity HPLC system (Agilent Technologies, Waldbronn, Germany) equipped with a 150 × 2.1 mm Sequant ZIC-pHILIC column with 5 μm particle size and an appropriate 20 × 2.1 mm precolumn (Merck, Darmstadt, Germany) which were both maintained at 40°C. For LC separation 10 mM ammonium acetate buffer (pH 9.2) was used as buffer A, whereas buffer B was acetonitrile. Before each injection the column was equilibrated for 15 min at 90% B. Injection volume was 5 μL for all analyses.

The LC-eluent was coupled to an ESI-QqTOF MS (TripleTOF 6600, AB Sciex, Darmstadt, Germany) equipped with an IonDrive ion source. The data acquisition was performed using Analyst TF 1.7 (AB Sciex, Concord, ON, Canada). Sugar phosphates and organic acids were measured in negative ionization mode in high sensitivity mode. For each $[M-H]^-$ precursor ion all Q1 windows corresponding to its carbon labeling states were monitored. For sugar phosphates and organic acids the following gradient was applied: 0 min: 90% B, 1 min: 90% B, 10 min: 70% B, 25 min: 65% B, 35 min: 10% B, 45 min: 10% B, 55 min: 10% B.

Amino acids were measured in positive ionization mode in High Sensitivity Mode. To elute amino acids the following gradient was applied: 0 min: 90% B, 1 min: 85% B, 12 min: 80% B, 18 min: 60% B, 25 min: 10% B, 35 min: 10% B, 45 min: 90% B. Again all Q1 isolation windows corresponding to the $[M+H]^+$ ions were monitored in high sensitivity mode.

MultiQuant 3.0.2 was used for extraction and integration of ion chromatograms. For each targeted fragment ion, the XICs of all its admissible carbon labeling states in each Q1 window were extracted. The targeted fragment ions for each metabolite and their structural identity was taken from.[34]

2.7 | Data processing and visualization

Data was stored, processed, and visualized using Microsoft Excel 2016 and Python 3.8, together with the packages numpy,[35] pandas,[36] and matplotlib.[37]

3 | RESULTS AND DISCUSSION

3.1 | *C. glutamicum* WMB2$_{evo}$ accumulates α-ketoglutarate and succinate during dynamic microaerobic cultivation on D-xylose

C. glutamicum is a known producer of organic acids under microaerobic and anaerobic conditions, where it switches from aerobic respiration to fermentative metabolism. While the predominant product under these conditions is L-lactate, extracellular accumulation of acetate and succinate also occurs, but to a lesser extent. This property has been successfully exploited in the past to establish production processes for L-lactate [26] and succinate.[14]

Most studies about fermentative processes in *C. glutamicum* deal with the wild type (ATCC 13032) and D-glucose as carbon and energy source, which enters the catabolism via glucose-6-phosphate as first intermediate of the Embden-Meyerhof-Parnas pathway (EMP). Strain WMB2$_{evo}$ on the other hand carries a functional Weimberg pathway for utilizing D-xylose as sole carbon and energy source for aerobic growth (Figure 1A). Here carbon enters the catabolism at the α-ketoglutarate node and is further metabolized via the TCA cycle, leading to a potential excess of NADH. Therefore, we questioned whether this strain can utilize D-xylose for growth under oxygen limiting conditions, and how the resulting phenotype differs from that of the *C. glutamicum* wild type on D-glucose.

To answer this question, a microaerobic batch cultivation with WMB2$_{evo}$ using defined CGXII medium with D-xylose as sole carbon and energy source was performed (Figure 1B). The cultivation conditions were deliberately chosen so that the culture was no longer sufficiently supplied with oxygen after reaching a certain biomass concentration. During the first 14 h, sufficient oxygen was present for unlimited aerobic growth (phase I). This was followed by a microaerobic growth phase (phase II). Dissolved oxygen concentration was 0%, indicating oxygen limitation, but cells continued to grow. During this phase, α-ketoglutarate, succinate, and acetate were formed. In phase III, cell growth stopped, even though substrate was still present, indicating a severe oxygen limitation. Despite this, succinate production even accelerated, and at the end of the cultivation, no more acetate could be found in the supernatant. Most likely it was taken up again, indicated by the dip in the dissolved oxygen signal at $t = 61$ h.

This first experiment revealed that D-xylose is utilized by strain WMB2$_{evo}$ under microaerobic conditions. The metabolic footprint differs from growth on D-glucose: α-ketoglutarate and succinate, both intermediates of the TCA cycle (Figure 1B), were accumulated at the end of the cultivation with titers of 0.83 and 28.64 mmol, respectively. The rate of their formation depended on the availability of oxygen. Acetate was formed as a by-product but was also taken up again as soon as oxygen limitation was removed. Noteworthy, no L-lactate could be found in the supernatant samples, which is a significant difference from the wild type strain under such conditions. Furthermore, no D-xylonate was found as a by-product of D-xylose utilization via the Weimberg pathway.[28]

3.2 | Verification of D-xylose utilization mode by ^{13}C-isotope labeling

The biosynthesis of α-ketoglutarate and succinate by oxidation of D-xylose via the Weimberg pathway is associated with the generation of excess energy equivalents, for example, 3 mol NADH and 1 mol ATP per mol of D-xylose in the case of succinate (cf. Figure 1A). Especially

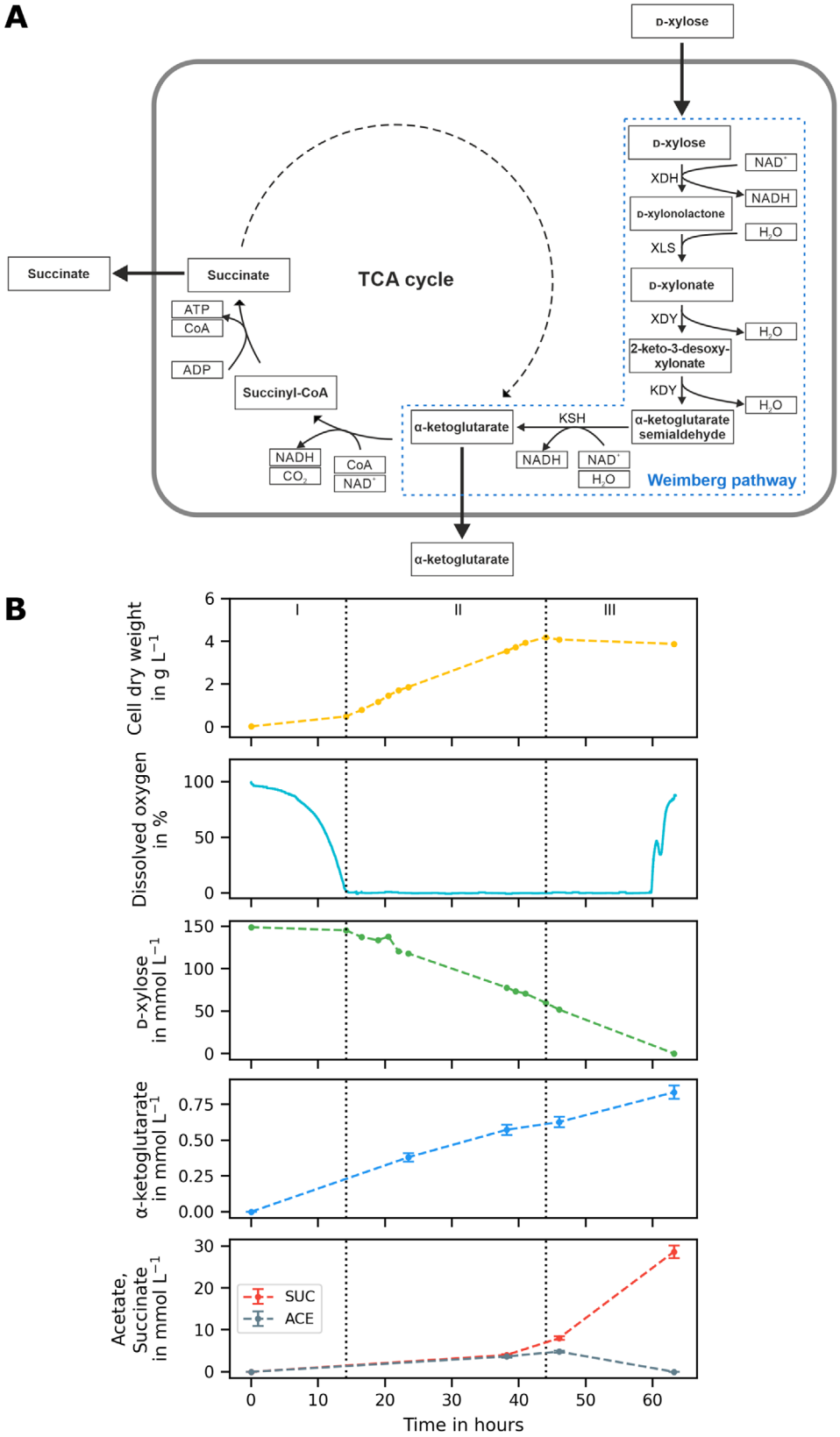

FIGURE 1 (A) Utilization of D-xylose via the Weimberg pathway. D-Xylose is converted to α-ketoglutarate without carbon loss and then further metabolized via the TCA cycle. Enzymes in the Weimberg pathway: xylose dehydrogenase (XDH), xylono-1,4-lactonase (XLS), xylonate dehydratase (XDY), 2-keto-3-xylonate dehydratase (KDY), α-ketoglutarate semialdehyde dehydrogenase (KSH). (B) Microaerobic batch cultivation of *C. glutamicum* WMB2$_{evo}$. The cultivation was done using a lab-scale 1 L bioreactor and defined CGXII medium containing 150 mmol L^{-1} D-xylose as sole carbon source and energy source. Microaerobic conditions were achived by a fixed stirrer rate of 400 rpm.

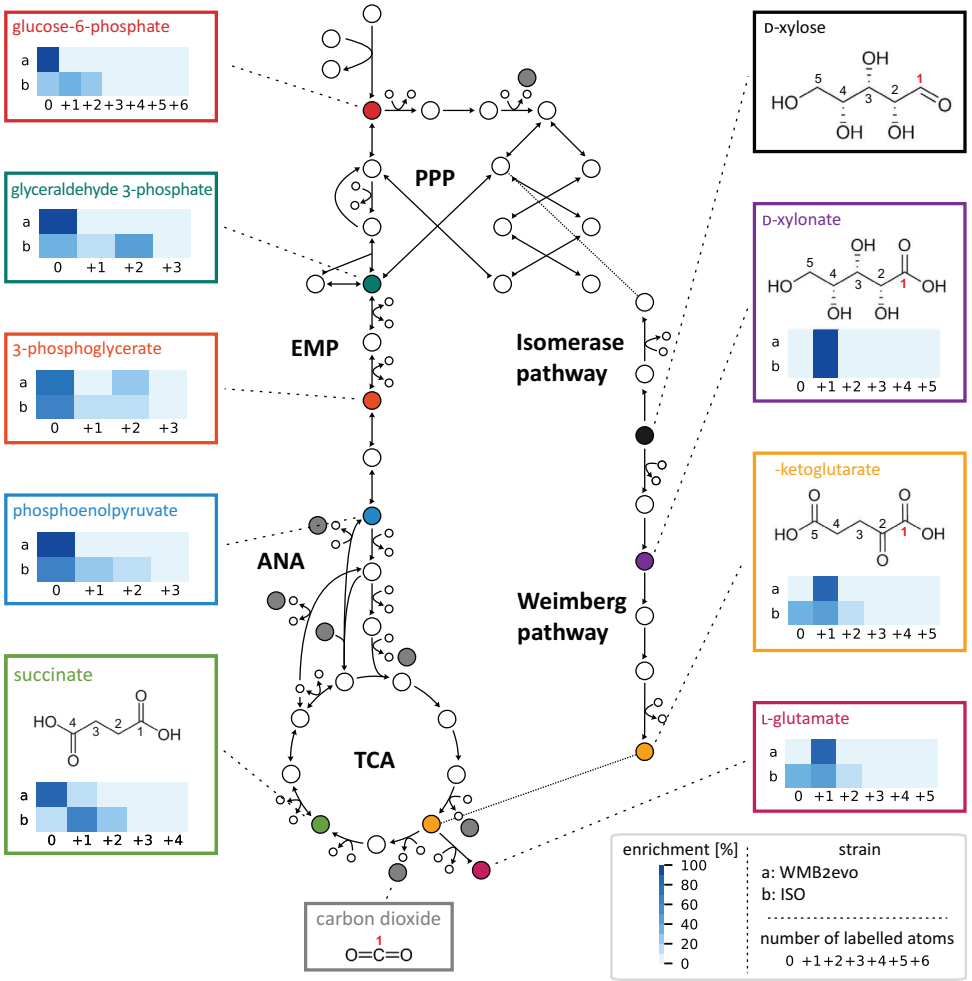

FIGURE 2 ^{13}C-labeling patterns of selected metabolites in strains a) *C. glutamicum* WMB2$_{evo}$ and b) *C. glutamicum* ISO following assimilation of 1-^{13}C-D-xylose as sole carbon and energy source. The position of the ^{13}C atom is highlighted in red.

under the microaerobic conditions applied, it is questionable whether this excess is fully utilized by the cells for growth and maintenance. As an alternative explanation, it is conceivable that another by-product is formed that allows cofactor recycling and that was not detectable by the applied analytics. As a second hypothesis, one could speculate on a different, previously unknown mode of D-xylose assimilation in the evolved WMB2$_{evo}$ strain, linking the formation of succinate to a reductive operation of the TCA cycle, as is the case in the wild type under microaerobic conditions.

To verify the exclusive operation of the Weimberg pathway for D-xylose assimilation in WMB2$_{evo}$, an isotope labeling experiment was performed. 1-^{13}C-D-xylose was used as the isotopic tracer and the resulting α-ketoglutarate pool should consist mainly of the isotopomer with a labeled carbon atom at the first position. In addition, succinate should be found mainly unlabeled, because the labeled carbon atom is released as CO_2 upon oxidation of α-ketoglutarate to succinyl-CoA. For a direct comparison of the resulting labeling patterns, a *C. glutamicum* strain that utilizes D-xylose via the isomerase pathway (ISO)[30] was analyzed in parallel. A much broader distribution of labeled carbon was expected for this strain, as D-xylose is introduced into the pentose phosphate pathway (PPP) at the xylulose-5-phosphate level and further metabolized via the oxidative PPP and the lower EMP (cf. Figure 2).

The experiment was performed with shake flask cultures sampled in the mid-exponential phase. Cold methanol quenching in combination with tandem mass spectrometry was performed to analyze the labeling patterns of key intracellular metabolites (Figure 2). As expected, the pools of D-xylonate, α-ketoglutarate, and L-glutamate in strain WMB2$_{evo}$ consisted mainly of the single labeled isotopomer (>89%) introduced by the substrate 1-^{13}C-D-xylose. Furthermore, succinate was predominantly unlabeled. However, a small portion of this pool (12%) also contained a single labeling that was higher than the natural isotopic abundance (≈4.5%). A likely explanation is that anaplerotic reactions present in *C. glutamicum* can recapture labeled carbon that is released as CO_2 in the reaction leading to succinyl-CoA. This could also explain the other smaller fractions of labeled 3-phosphoglycerate and glyceraldehyde-3-phosphate (cf. Figure 2). By contrast, in the ISO strain only D-xylonate shows a narrow labeling pattern, proving that D-xylonate is also formed from D-xylose in this strain. This is in good agreement with the previous finding that the endogenous enzyme IolG

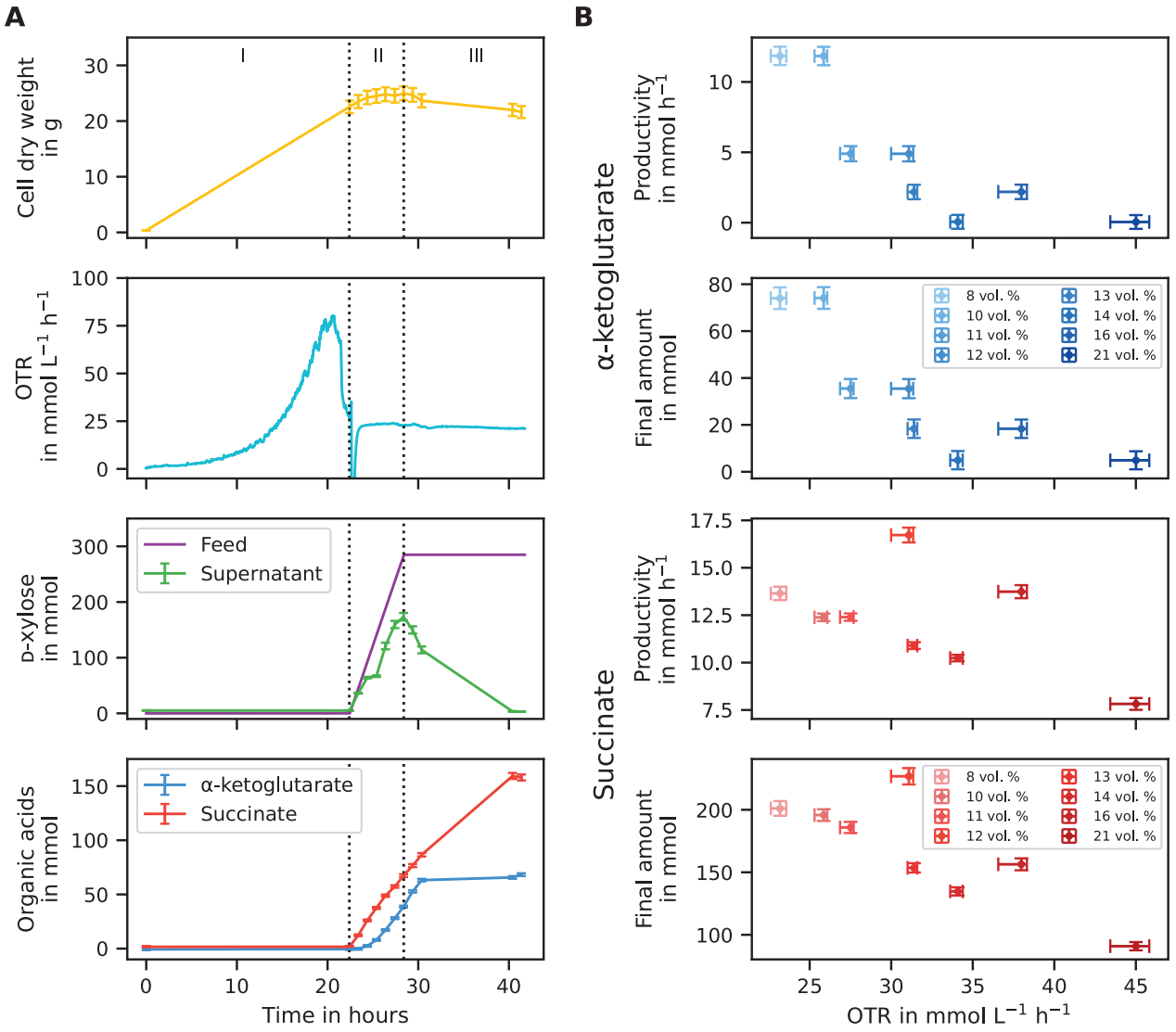

FIGURE 3 Impact of oxygen availability on α-ketoglutarate and succinate productivity. (A) Exemplary bioreactor screening process using *C. glutamicum* $WMB2_{evo}$ and defined CGXII medium. In phase I, biomass was generated using 40 g of D-glucose as sole carbon and energy source. In phase II, microaerobic conditions were induced by fixing the stirrer rate to 900 rpm, the aeration rate to 0.2 vvm, and varying the oxygen content in the inlet gas. As substrate for the co-production of both organic acids, D-xylose was fed into the bioreactor via a peristaltic pump at a rate of 48 mmol h^{-1} for 6 h. In phase III, the feed was stopped and monitoring continued. (B) Productivity and titers of all eight bioreactor screening processes. The oxygen concentration in the inlet gas was varied between 8 and 21 vol.%, resulting in an oxygen transfer rate plotted on the X-axis. Productivity was calculated by linear regression of the data points within each production phase. No productivity could be calculated for α-ketoglutarate for the 14 and 21 vol.% conditions because no production phase could be defined.

also drives D-xylose oxidation in *C. glutamicum*.[38] In summary, the labeling pattern found for *C. glutamicum* $WMB2_{evo}$ verifies the exclusive utilization of D-xylose via the Weimberg pathway in this strain.

3.3 | Impact of oxygen availability on organic acid production performance

To further investigate, the influence of oxygen availability on the co-production of α-ketoglutarate and succinate, a dedicated microaerobic fed-batch screening process was set up (Figure 3A). In phase I, biomass was produced using a defined amount of D-glucose and fully aerobic conditions ensured by DO-controlled stirring and gassing with pure air. From phase II onwards, microaerobic conditions were achieved by lowering the stirring speed as well as the volumetric gas flow rate and mixing nitrogen into the inlet gas. Depending on the proportion of nitrogen added, the oxygen supply could be varied in a controlled manner. In phase II, D-xylose was also added as a substrate for organic acid production. In this procedure, only α-ketoglutarate and succinate were produced in quantifiable amounts; acetate production was absent. This is likely due to the rapid change between fully aerobic and microaerobic conditions in this setup, which also leads to growth decoupling of the production process. In phase III, the supply of D-xylose was stopped, but since not all D-xylose was taken up by the cells at this

time, organic acid production continued. Interestingly, the accumulation of α-ketoglutarate stopped rapidly after the termination of feeding, whereas the production of succinate continued until all the D-xylose was used up.

In total, eight different levels of oxygen percentage in the inlet gas flow were tested (Figure 3B, Figures S1–S3). The resulting OTRs ranged from 22 to 45 mmol L^{-1} h^{-1}. For α-ketoglutarate, the highest amount, 74.0 mmol, was achieved by the processes with the lowest and second lowest oxygen levels. The same processes also reached the highest productivities of 11.85 and 11.84 mmol h^{-1}, respectively. For succinate both the highest amount, 226.8 mmol, and the highest productivity, 16.7 mmol h^{-1}, were achieved by the processes with 12 vol.%.

A general trend seems to be that a higher degree of oxygen limitation leads to higher α-ketoglutarate titers and productivities. This is in good agreement with the first experiment (cf. Figure 1A). Little to no α-ketoglutarate was found under the higher oxygen conditions. It is noteworthy that varying the oxygen supply does not cause a shift in the carbon flux between the two organic acids, but rather a lower oxygen supply results in a higher amount of both products. Carbon balances revealed that a substantial amount of carbon is still converted to CO_2, hinting to the need for further strain optimization. Note, the validity of carbon balances for these processes could be limited due to issues regarding CO_2 measurement (Figures S2 and S3).

In conclusion, the screening experiments showed that α-ketoglutarate and succinate can be produced in a growth-decoupled manner. Lower oxygen availability increased the accumulation of α-ketoglutarate and succinate, but below an OTR of 30 mmol L^{-1} h^{-1} productivity for succinate began to decline.

3.4 | Process intensification by evaluation of different feeding strategies

Based on previous findings, two strategies for enhanced co-production of α-ketoglutarate and succinate were evaluated: A fed-batch process with an extended feed phase and a pulsed fed-batch in which D-xylose is rapidly added at discrete time points. Because of the growth-decoupled production mode, potential substrate inhibition was assumed to be less critical, so high D-xylose concentrations were used. A total of 1440 mmol (reactors 1, 2, and 3) and 720 mmol (reactor 4) were added. For all reactors, biomass was generated as described before.

Continuous feeding resulted in a linear increase of α-ketoglutarate in the supernatant, shortly after feeding was started (Figure 4A, Figure S4, and Table 1). Production occurred throughout the feeding phase and beyond, resulting in an accumulation of 140 mmol (R1) and 146 mmol (R2) α-ketoglutarate, respectively. The rate of product formation remained constant throughout the production phase, indicating that no inhibition occurred with this feeding regimen. Succinate also accumulated rapidly but reached a maximum at $t = 68$ h with amounts of 190 mmol (R1) and 160 mmol (R2), respectively.

Pulsed feeding also resulted in accumulation of α-ketoglutarate and succinate (Figures 4B and S4, and Table 1). Compared with continuous feeding, the accumulation of α-ketoglutarate was faster at the beginning, indicating a positive effect of the high substrate concentrations. In reactor 3 fed with 1440 mmol D-xylose, a slightly lower amount of 128 mmol α-ketoglutarate was produced, compared to continuous feeding. However, due to the lower amount of base added to this reactor, the titer is higher. Reactor 4 received only a 720 mmol substrate pulse. Nevertheless, more than half the amount of α-ketoglutarate (75 mmol) was produced, indicating possible product inhibition. Succinate accumulated at similar rates compared with continuous feeding. Interestingly, accumulation also stopped at similar amounts, and there was little difference between reactor 3 (two pulses) and reactor 4 (one pulse). Probably, the cells were not able to export more succinate under these process conditions. With this feeding mode, biomass decreased significantly during the production phase, an effect that was not as pronounced with continuous feeding and could explain the lower amount of base added.

For all processes, yields for α-ketoglutarate and succinate were in the range of 0.05 — 0.14 mol mol^{-1}, meaning that only 15 — 24% of the substrate was converted to the target products. Additionally, carbon balances showed a substantial gap between carbon input and carbon quantified (Figure S4). It is therefore likely, that at least one other by-product was formed. For example, the amino acid L-glutamate, which is directly derived from α-ketoglutarate, could accumulate intracellularly. It is known that *C. glutamicum* is able to store large amounts of this amino acid intracellularly,[39,40] and the required reduction of α-ketoglutarate might also be driven by an excess of NADH.

TABLE 1 Performance indicators for α-ketoglutarate and succinate co-production by applying either constant feed or pulses

Reactor	R1	R2	R3	R4
Feed	Constant	Constant	Two Pulses	One Pulse
Substrate [$mmol_{Xyl}$]	1440	1440	1440	720
Residual substrate [$mmol_{Xyl}$]	80.5	107.4	31.5	0
	α-ketoglutarate			
Titer [$mmol_{AKG}$ L^{-1}]	67.3	71.3	78.4	45.6
Amount [$mmol_{AKG}$]	139.8	146.1	128.3	73.0
Yield [$mmol_{AKG}$ $mmol_{Xyl}^{-1}$]	0.10	0.11	0.09	0.05
Space time yield [$mmol_{AKG}$ L^{-1} h^{-1}]	1.0	1.1	1.2	0.7
	Succinate			
Titer [$mmol_{Suc}$ L^{-1}]	91.3	77.3	96.2	92.5
Amount [$mmol_{Suc}$]	189.4	158.2	157.6	144.3
Yield [$mmol_{Suc}$ $mmol_{Xyl}^{-1}$]	0.14	0.12	0.11	0.10
Space time yield [$mmol_{Suc}$ L^{-1} h^{-1}]	1.4	1.2	1.5	1.4

Space time yield was calculated from start of feeding until the end of the cultivation.

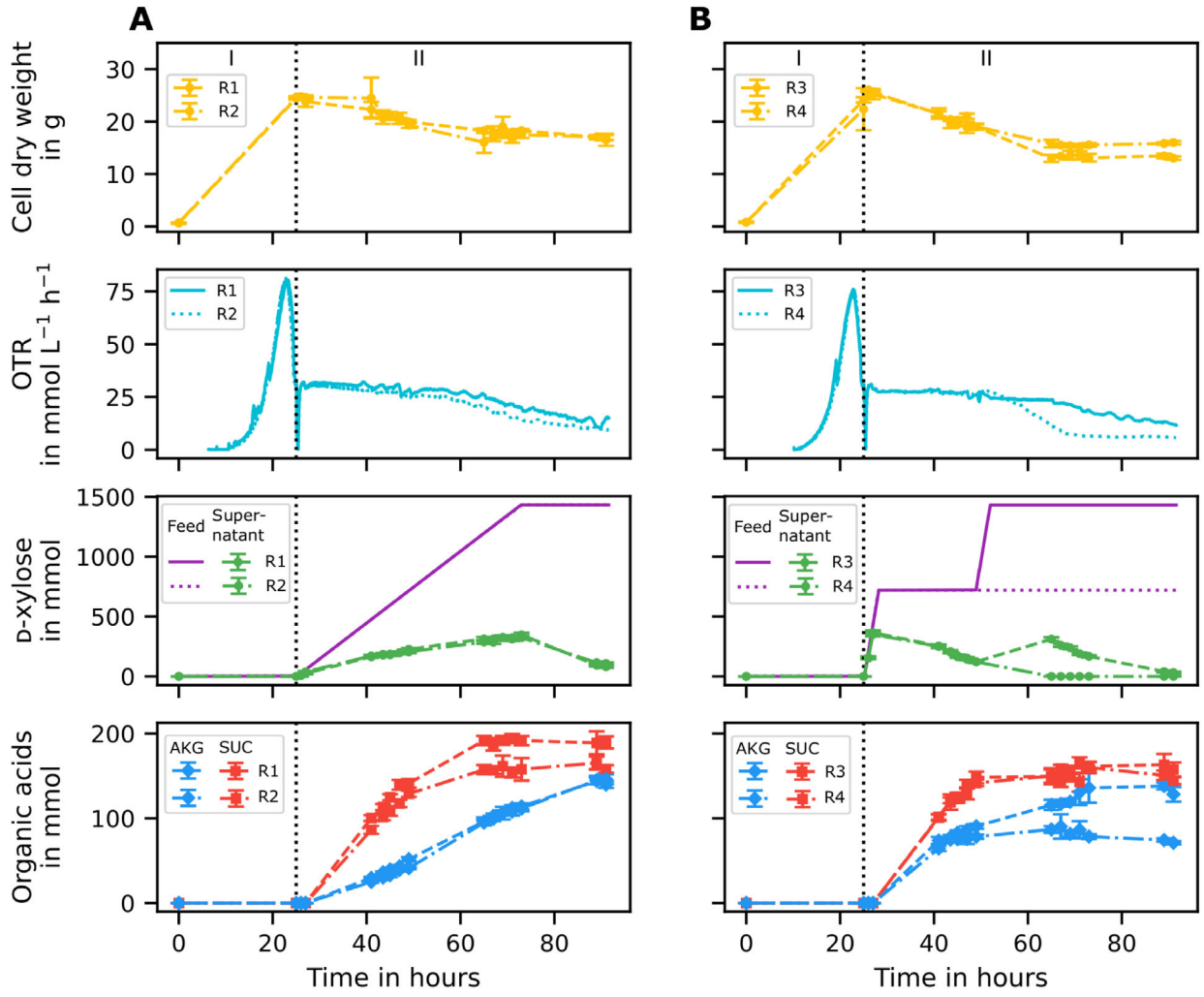

FIGURE 4 Evaluation of different feeding strategies for enhanced co-production of α-ketoglutarate and succinate. (A) Fed-batch bioreactor process using *C. glutamicum* WMB2$_{evo}$ and defined CGXII medium. In phase I, biomass was produced using 40 g of D-glucose as sole carbon and energy source. In phase II, microaerobic conditions were induced by fixing the stirrer rate to 900 rpm, the aeration rate to 0.2 vvm, and the oxygen content in the inlet gas to 12 vol.%. As substrate for α-ketoglutarate production, D-xylose was fed into the bioreactor via a peristaltic pump with at a rate of 48 mmol h^{-1} for 30 h. (B) Pulsed fed-batch bioreactor process using *C. glutamicum* WMB2$_{evo}$ and defined CGXII medium. Biomass production and microaerobic conditions were identical to A. Substrate addition was in pulses, with reactor 3 receiving two pulses of 720 mmol D-xylose and reactor 4 receiving one pulse of 720 mmol D-xylose.

Testing of different feeding strategies revealed that high substrate concentrations lead to higher product formation rates, but possibly also to higher byproduct accumulation. In addition, despite growth-decoupled production, cells were more affected by pulsed feeding than by continuous feeding. Pulsed feeding resulted in slightly higher titers for both α-ketoglutarate and succinate, which may be beneficial for downstream applications. Moreover, pulsed feeding could be performed using the substrate as solid, further reducing dilution and potentially increasing product titers.

4 | CONCLUSIONS

Despite not being optimized for that purpose, *C. glutamicum* WMB2$_{evo}$ is able to co-produce substantial amounts of α-ketoglutarate and succinate from the highly abundant lignocellulosic sugar D-xylose. By screening different microaerobic conditions and feeding strategies, titers of up to 78.4 mmol L^{-1} (11.45 g L^{-1}) for α-ketoglutarate and 96.2 mmol L^{-1} (11.36 g L^{-1}) for succinate were reached in a growth-decoupled process.

It is most likely that these performance indicators can be further improved by metabolic engineering, for example, by improving D-xylose uptake[41,42] or reducing by-product formation. Future work will focus on tailor-made down-stream processing of both organic acids from the fermentation broth to enable their application as building blocks in chemical syntheses. Alternatively, direct conversion of one or both acids via whole-cell or cell-free enzymatic approaches can be envisioned; thus, extending the network of value chains starting from cheap and renewable lignocellulosic feedstocks.

ACKNOWLEDGMENTS

The authors acknowledge the financial support of the Bioeconomy Science Center as part of the project HyImPAct ("Hybrid processes for Important Precursor and Active pharmaceutical ingredients"). The scientific activities of the Bioeconomy Science Center were financially supported by the Ministry of Innovation, Science and Research within the framework of the NRW Strategieprojekt BioSC (no. 313/323-400-002 13).

Open access funding enabled and organized by Projekt DEAL.

CONFLICT OF INTEREST

The authors declare no conflict of interest.

AUTHOR CONTRIBUTIONS

Niklas Tenhaef coordinated, planned, performed, and supervised experiments, performed data analysis and visualization, and wrote the paper. Jannick Kappelmann planned the ^{13}C labeling experiment, supervised sample preparation procedures, performed data acquisition, and supervised data analysis. Arabel Eich performed the ^{13}C labeling experiment including data analysis. Marc Weiske and Lisette Brieß performed bioreactor experiments, sample preparation, and data analysis. Christian Brüsseler, Jan Marienhagen, and Wolfgang Wiechert discussed the data and helped to finalize the manuscript. Stephan Noack coordinated, planned, and supervised experiments as well as data analysis and wrote the paper.

DATA AVAILABILITY STATEMENT

The data used in this study can be made available upon reasonable request to the corresponding author.

ORCID

Stephan Noack https://orcid.org/0000-0001-9784-3626

REFERENCES

1. Rubin, E. M. (2008). Genomics of cellulosic biofuels. *Nature*, *454*, 841–845.
2. Van Wyk, J. P. (2001). Biotechnology and the utilization of biowaste as a resource for bioproduct development. *Trends in Biotechnology.*, *19*, 172–177.
3. Sauer, M., Porro, D., Mattanovich, D., & Branduardi, P. (2008). Microbial production of organic acids: Expanding the markets. *Trends in Biotechnology.*, *26*, 100–108.
4. Schaffer, S., Grammann, K., & Reinecke, L. (2018). Acyl amino acid production, *WO2016165968A1*, Evonik Operations GmbH.
5. Otto, C., Yovkova, V., & Barth, G. (2011). Overproduction and secretion of α-ketoglutaric acid by microorganisms. *Applied Microbiology and Biotechnology.*, *92*, 689–695.
6. Stottmeister, U., Aurich, A., Wilde, H., & Andersch, J. (2005). White biotechnology for green chemistry: Fermentative 2-oxocarboxylic acids as novel building blocks for subsequent chemical syntheses. *Journal of Industrial Microbiology & Biotechnology.*, *32*, 651–664.
7. Barrett, D. G., & Yousaf, M. N. (2008). Poly(triol α-ketoglutarate) as biodegradable, chemoselective, and mechanically tunable elastomers. *Macromolecules*, *41*, 6347–6352.
8. Förster, A., Mauersberger, S., Köllner, K., & Barth, G. (2006). *Verbundvorhaben: Biotechnologische Gewinnung von Carbonsäuren, Teilvorhaben 3: Genetic engineering oxocarbonsäurebildender Hefen*, Endbericht; Projekt der Fachagentur für nachwachsende Rohstoffe eV FZ: 22002505.
9. Verseck, S., Karau, A., & Weber, M. (2009). Fermentative production of alpha-ketoglutaric acid, *WO2009053489A1*, Evonik-Degussa GmbH.
10. Ahn, J. H., Jang, Y.-S., & Lee, S. Y. (2016). Production of succinic acid by metabolically engineered microorganisms. *Current Opinion in Biotechnology.*, *42*, 54–66.
11. Choi, S., Song, C. W., Shin, J. H., & Lee, S. Y. (2015). Biorefineries for the production of top building block chemicals and their derivatives. *Metabolic Engineering.*, *28*, 223–239.
12. Hong, U. G., Park, H. W., Lee, J., & Hwang, S. (2012). Hydrogenation of succinic acid to tetrahydrofuran (THF) over rhenium catalyst supported on H_2SO_4-treated mesoporous carbon. *Applied Catalysis A*, *415*, 141–148.
13. Xu, J., & Guo, B.-H. (2010). Microbial Succinic Acid, Its Polymer Poly(butylene succinate), and Applications, in: Chen, G. G.-Q. (Ed.), *Plastics from Bacteria: Natural Functions and Applications*, Springer, Berlin Heidelberg, Berlin, Heidelberg, pp. 347–388.
14. Litsanov, B., Brocker, M., & Bott, M. (2012). Toward homosuccinate fermentation: Metabolic engineering of *Corynebacterium glutamicum* for anaerobic production of succinate from glucose and formate. *Applied and Environmental Microbiology.*, *78*, 3325–3337.
15. Jiang, M., Ma, J., Wu, M., Liu, R., Liang, L., Xin, F., Zhang, W., Jia, H., & Dong, W. (2017). Progress of succinic acid production from renewable resources: Metabolic and fermentative strategies. *Bioresource Technology.*, *245*, 1710–1717.
16. Li, C., Yang, X., Gao, S., Wang, H., & Lin, C. S. K. (2017). High efficiency succinic acid production from glycerol via in situ fibrous bed bioreactor with an engineered *Yarrowia lipolytica*. *Bioresource Technology*, *225*, 9–16.
17. Liu, R., Liang, L., Cao, W., Wu, M., Chen, K., Ma, J., Jiang, M., Wei, P., & Ouyang, P. (2013). Succinate production by metabolically engineered *Escherichia coli* using sugarcane bagasse hydrolysate as the carbon source. *Bioresource Technology*, *135*, 574–577.
18. Liu, W., Zheng, P., Yu, F., & Yang, Q. (2015). A two-stage process for succinate production using genetically engineered *Corynebacterium acetoacidophilum*. *Process Biochemistry*, *50*, 1692–1700.
19. Sawisit, A., Jantama, K., Zheng, H., Yomano, L. P., York, S. W., Shanmugam, K. T., & Ingram, L. O. (2015). Mutation in galP improved fermentation of mixed sugars to succinate using engineered *Escherichia coli* AS1600a and AM1 mineral salts medium. *Bioresource Technology*, *193*, 433–441.
20. Akhtar, J., Idris, A., & Aziz, R. A. (2014). Recent advances in production of succinic acid from lignocellulosic biomass. *Applied Microbiology Biotechnology*, *98*, 987–1000.
21. Chen, K., Jiang, M., Wei, P., Yao, J., & Wu, H. (2010). Succinic acid production from acid hydrolysate of corn fiber by *Actinobacillus succinogenes*. *Applied Biochemistry and Biotechnology.*, *160*, 477–485.
22. Weimberg, R. (1961). Pentose oxidation by *Pseudomonas fragi*. *Journal of Biological Chemistry.*, *236*, 629–635.
23. De Bhowmick, G., Sarmah, A. K., & Sen, R. (2018). Lignocellulosic biorefinery as a model for sustainable development of biofuels and value added products.*Bioresource Technology*, *247*, 1144–1154.
24. Ekman, A., Wallberg, O., Joelsson, E., Börjesson, P., Possibilities for sustainable biorefineries based on agricultural residues–a case study of potential straw-based ethanol production in Sweden. *Applied Energy* 2013, *102*, 299–308.
25. Viikari, L., Vehmaanperä, J., Koivula, A. (2012) Lignocellulosic ethanol: From science to industry. *Biomass Bioenergy*, *46*, 13–24.
26. Okino, S., Suda, M., Fujikura, K., Inui, M., & Yukawa, H. (2008). Production of D-lactic acid by *Corynebacterium glutamicum* under oxygen deprivation. *Applied Microbiology and Biotechnology.*, *78*, 449–454.
27. Radek, A., Krumbach, K., Gätgens, J., & Wendisch, V. F. (2014). Engineering of *Corynebacterium glutamicum* for minimized carbon loss

during utilization of D-xylose containing substrates. *Journal of Biotechnology.*, *192*, 156–160.
28. Radek, A., Tenhaef, N., Müller, M. F., Brüsseler, C., Wiechert, W., Marienhagen, J., Polen, T., & Noack, S. (2017). Miniaturized and automated adaptive laboratory evolution: Evolving *Corynebacterium glutamicum* towards an improved D-xylose utilization. *Bioresource Technology*, *245*, 1377–1385.
29. Brüsseler, C., Späth, A., Sokolowsky, S., & Marienhagen, J. (2019). Alone at last! - Heterologous expression of a single gene is sufficient for establishing the five-step Weimberg pathway in *Corynebacterium glutamicum*. *Metabolic Engineering Communications*, *9*.
30. Meiswinkel, T. M., Gopinath, V., Lindner, S. N., Nampoothiri, K. M., & Wendisch, V. F. (2013). Accelerated pentose utilization by *Corynebacterium glutamicum* for accelerated production of lysine, glutamate, ornithine and putrescine. *Microbial Biotechnology*, *6*, 131–140.
31. Keilhauer, C., Eggeling, L., & Sahm, H. (1993). Isoleucine synthesis in *Corynebacterium glutamicum*: Molecular analysis of the ilvB-ilvN-ilvC operon. *Journal of Bacteriology.*, *175*, 5595–5603.
32. Hemmerich, J., Tenhaef, N., Steffens, C., Kappelmann, J., Weiske, M., Baumgart, M., Rückert, C., Ruwe, M., Siebert, D., Wendisch, V. F., Kalinowski, J., Wiechert, W., & Oldiges, M. (2018). Less sacrifice, more insight: Repeated low-volume sampling of microbioreactor cultivations enables accelerated deep phenotyping of microbial strain libraries. *Biotechnology Journal.*, *14*.
33. Kallscheuer, N., Vogt, M., Kappelmann, J., Krumbach, K., Noack, S., Bott, M., & Marienhagen, J. (2015). Identification of the phd gene cluster responsible for phenylpropanoid utilization in *Corynebacterium glutamicum*. *Applied Microbiology and Biotechnology.*, *100*, 1871–1881.
34. Kappelmann, J., Klein, B., Geilenkirchen, P., & Noack, S. (2017). Comprehensive and accurate tracking of carbon origin of LC-tandem mass spectrometry collisional fragments for ^{13}C-MFA. *Analytical and Bioanalytical Chemistry.*, *409*, 2309–2326.
35. Harris, C. R., Millman, K. J., van der Walt, S. J., Gommers, R., Virtanen, P., Cournapeau, D., Wieser, E., Taylor, J., Berg, S., Smith, N. J., Kern, R., Picus, M., Hoyer, S., van Kerkwijk, M. H., Brett, M., Haldane, A., Del Río, J. F., Wiebe, M., Peterson, P., Gérard-Marchant, P., … Oliphant, T. E. (2020). Array programming with NumPy. *Nature*, *585*, 357–362.
36. McKinney, W. (2011). Pandas: A foundational Python library for data analysis and statistics. *Python for High Performance Scientific Computing*, *14*, 1–9.
37. Hunter, J. D. (2007). Matplotlib: A 2D graphics Environment. *Computing in Science & Engineering.*, *9*, 90–95.
38. Tenhaef, N., Brüsseler, C., Radek, A., Hilmes, R., Unrean, P., Marienhagen, J., & Noack, S. (2018). Production of D-xylonic acid using a non-recombinant *Corynebacterium glutamicum* strain. *Bioresource Technology.*, *268*, 332–339.
39. Skjerdal, O. T., Sletta, H., Flenstad, S. G., Josefsen, K. D., Levineet, D. W., & Ellingsen, T. E. (1995). Changes in cell volume, growth and respiration rate in response to hyperosmotic stress of NaCl, sucrose and glutamic acid in *Brevibacterium lactofermentum* and *Corynebacterium glutamicum*. *Applied Microbiology and Biotechnology.*, *43*, 1099–1106.
40. da Luz, J. A., Hans, E., Frank, D., & Zeng, A.-P. (2017). Analysis of intracellular metabolites of *Corynebacterium glutamicum* at high cell density with automated sampling and filtration and assessment of engineered enzymes for effective L-lysine production. *Engineering in Life Sciences.*, *17*, 512–522.
41. Sasaki, M., Jojima, T., Kawaguchi, H., Inui, M., & Yukawa, H. (2009). Engineering of pentose transport in *Corynebacterium glutamicum* to improve simultaneous utilization of mixed sugars. *Applied Microbiology and Biotechnology*, *85*, 105–115.
42. Pérez-García, F., & Wendisch, V. F. (2018). Transport and metabolic engineering of the cell factory *Corynebacterium glutamicum*. *FEMS Microbiology Letters*, *365*, fny166.

SUPPORTING INFORMATION

Additional supporting information may be found online in the Supporting Information section at the end of the article.

How to cite this article: Tenhaef, N., Kappelmann, J., Eich, A., Weiske, M., Brieß, L., Brüsseler, C., Marienhagen, J., Wiechert, W., & Noack, S. (2021). Microaerobic growth-decoupled production of α-ketoglutarate and succinate from xylose in a one-pot process using *Corynebacterium glutamicum*. *Biotechnol. J*, e2100043. https://doi.org/10.1002/biot.202100043